PHILOSOPHICAL TRANSACTIONS OF THE ROYAL SOCIETY A MATHEMATICAL, PHYSICAL & ENGINEERING SCIENCES

Limit Analysis of Plates and Isoperimetric Inequalities

J. D. Allen, I. F. Collins and P. G. Lowe

Phil. Trans. R. Soc. Lond. A 1994 **347**, 113-137
doi: 10.1098/rsta.1994.0041

Limit analysis of plates and isoperimetric inequalities†

By J. D. Allen, I. F. Collins and P. G. Lowe
School of Engineering, University of Auckland, Private Bag 92019, Auckland, New Zealand

A general isoperimetric inequality for the collapse loads of uniformly loaded, edge supported rigid-plastic plates of arbitrary shape is established. The inequality provides a lower bound to this load and involves just the length of the perimeter and the area of the collapsing region of the plate. This paper establishes a proof, under certain restrictions, of this inequality which to-date has been just a conjecture.

1. Introduction and perspective

In this paper we consider small deflection, rigid-plastic plate bending theory for isotropic, homogeneous, edge supported, simply connected, uniformly loaded plates exhibiting the material response described by the square yield locus and associated flow rule. The plates are analysed in the state of collapse, elastic deflections are ignored and only the simplest class of loading type and material response are being considered. Even given these simplifications, and at least 50 years of endeavour to solve the boundary value problems implied, it is perhaps strange that there is still a need to revisit the subject.

The main reason we see for this need is that so few boundary value problems have been solved. The situation may already be that no further new boundary value problems will be solved in detail. The problems considered by Fox (1974) may remain the only non-circular, clamped edge boundary value problems solved; at least with techniques involving the direct solution of the governing partial differential equations.

Some aspects of our subject can be traced back to Mariotte (1686), who published experimental findings relating to plate collapse. The concept of a mechanism of collapse for a structure is well illustrated by Moseley (1834) in his popular account of mechanics. There are no doubt other antecedents which could be cited. The effective beginning of the modern era in our subject is here taken to be the publication of the Johansen (1943) thesis entitled Brudlinieteorier (yield line theory). In this work, which is primarily devoted to analysing the collapse conditions for edge supported plates, Johansen made extensive use of the concepts of yield lines forming mechanisms for collapse. What is here referred to as the square yield locus should perhaps rightly be called the 'Johansen yield locus' since he proposed such a use in his thesis. The context for Johansen's yield lines arose from experiments on reinforced concrete slabs made by him and other Scandinavian and German workers, see Bach (1920).

By the time Johansen's thesis was presented he had been working at the subject

† Dedicated to the memory of Randal H. Wood (1913–1987).

Phil. Trans. R. Soc. Lond. A (1994) **347**, 113–137
Printed in Great Britain

for about 15 years and had published aspects of the theory earlier. Acceptance of the importance of these studies was slow, in part due to the inacessibility of the thesis. The stimulus to mechanics studies in general during and after World War II, combined with the re-establishment, most notably in America, of vigorous research schools in several Universities but in particular at Brown University, resulted in rapid advances in what became known as the limit theorems and applications of these concepts to a variety of problems. William Prager (1903–1980) was a central contributor to these advances. He and co-workers at Brown solved the circular plate at collapse, first for simple support and then with clamped support, in particular for the Tresca yield locus in Hopkins & Prager (1953). Schumann (1958*a*) while working at Brown, extended the concepts to plates of arbitrary shape, under a point load and with simple support. Schumann (1958*b*) also published a second paper in 1958 which has been seldom referenced, but which can be thought of as the starting point for the study undertaken in the present paper. In this paper he established an inequality for the collapse pressure of arbitrarily shaped, simply supported plates. It is particularly surprising that this second paper is not referenced in Prager's book (1959) on plasticity theory published shortly afterwards.

By far the greater amount of published research has been devoted to applying upper bound, mechanism-based, approximate analyses to plate collapse studies. Mansfield (1957) made notable advances by the use of curved log spiral yield lines in corner regions. Nielsen (1964), who succeeded Johansen in Copenhagen, published an important study in which several exact solutions for non-circular simply supported shapes were given.

Randal H. Wood (1913–1987) published his 'Plastic and elastic design of slabs and plates' in 1961. This work proved to be a valuable stimulus to further understanding of yield line theory. The MCR Special Publication (1965) followed soon afterwards. Massonnet (1967) published a useful survey of special types of exact solutions, some obtained by inverse methods. However, Wood (1968, 1969) himself began expressing doubts about the completeness of yield line theory and suggested that exact solutions might not be obtainable. He was probably inclined to this view because of the difficulty of solving exactly apparently simple problems such as the square clamped plate under uniform load. Fox (1974) disagreed and in due course succeeded in finding the exact solution to this boundary value problem. But the solution was perhaps unexpectedly complicated. Indeed, based upon this evidence, it can be concluded that few other exact solutions are likely to be discovered using such methods, especially where the boundary is clamped and the plate shape has corners. Recent comprehensive surveys of the limit analysis of plates in bending are contained in the texts by Nielsen (1984) and Sobotka (1989). The bulk of the discussion in both texts relates to upper bound analyses.

An attractive alternative procedure is to use linear programming or some other computational optimisation technique based on the plastic limit theorems, to obtain close upper and lower bounds on the collapse loads. The results of a number of such studies have been published (see, for example, Hodge & Belytschko 1968; Palmer 1970; Chan 1972; Christiansen 1980; Christiansen & Larsen 1983). However, these have yet to reach the stage of producing entirely reliable results (cf. Christiansen & Larsen 1983), and they also give little information of the nature of the collapse mechanism. It is likely therefore that the approximate 'engineering theories' based on yield-line theory or equivalently on upper bound mechanisms will continue to be the most widely used design tool.

Mention has already been made of the paper by Schumann (1958*b*). It was published during the period of most rapid development of the subject and established a result quite unlike other results of the period. Indeed we are not aware of any similar study until the book by Lowe (1982). The novelty in the paper by Schumann (1958*b*) was the establishment of a bound (inequality) on the collapse pressure for simply supported plates of *any shape*. Specifically, the result was that the total load acting on the deforming portion of the plate at collapse is never less than the total load acting on a circular plate of equal area. A circular shaped plate is hence the weakest shaped plate for a fixed area.

Unaware of Schumann's statement and proof of this result for simply supported plates 24 years earlier, Lowe (1982) conjectured results of similar type (here referred to as the *weak* conjecture) for edge supported plates, either simply supported or clamped. A further more stringent conjectured inequality (here referred to as the *strong* conjecture) was also proposed, which if true would ensure the truth of the weaker Schumann inequalities (Lowe 1982). Subsequent papers by Lowe (1984, 1988*a*–*c*) have explored the consequences of these strong conjectures being true. Thus far no inconsistencies have been found between the conjectures and known exact solutions. In particular, if the *strong* conjecture could be proved, then a procedure follows for obtaining lower bound estimates to collapse loads, where at present no constructive method is available for such bounds based purely on limit analysis principles. The present paper provides a proof of the stronger inequality and hence automatically of the Schumann inequality for edge supported plates, under certain restrictions.

We propose to dedicate this paper to the memory of Randal H. Wood (1913–1987). In addition to his contributions as noted above, he in a sense anticipated the contents of this paper in Wood (1961, p. 332, §91): 'Suggestions for future research, (b) dimensional analysis applied to slabs'. Though we have only recently become aware of his proposals there, his suggestion that an area/perimeter parameter may be important, is precisely the suggestion we are further exploring in this paper. Wood too seems to have been unaware of Schumann's paper.

As already stated the conjecture is concerned with the collapse pressure p of a *uniformly* loaded plate. The *strong* assertion made by Lowe (1982) is that for any collapse mechanism, the associated pressure satisfies the inequality,

$$pA/M \geqslant 3k(B^2/2A), \tag{1.1}$$

where M is the yield moment, A and B are respectively the plan area and the perimeter of the *collapsing zone of the plate*, which may or may not be the whole of the plate, and the parameter k is equal to 1 when the edges are simply supported and 2 for a plate with clamped edges.

From the celebrated classical isoperimetric inequality, we know that for any closed plane curve $B^2/A \geqslant 4\pi$, with equality for a circle, so that (1.1) implies the weaker inequality:

$$pA/M \geqslant 6\pi k. \tag{1.2}$$

Equality in (1.2) gives the known exact solution for simply supported and clamped circular plates. Both conjectures hence satisfy the requirement of a true isoperimetric inequality in that equality is actually attained for some member(s) of the class of problems for which the inequality holds (cf. Payne 1991). The second weaker inequality is that proved for simply supported plates by Schumann (1958*b*) using the

PHILOSOPHICAL TRANSACTIONS OF THE ROYAL SOCIETY A MATHEMATICAL, PHYSICAL & ENGINEERING SCIENCES

Schwarz symmetrization technique. This is one of the standard procedures for establishing such isoperimetric inequalities (Burago & Zalgaller 1980). (In fact Schumann actually used the Tresca failure criterion, but his analysis is readily modified for the square yield locus.)

The *strong* conjecture (1.1) can be written slightly differently as

$$(p/M) \geqslant (3k/2)(B/A)^2. \qquad (1.1)'$$

It follows that *if* this conjecture holds for *all* mechanisms, and hence includes those associated with the exact solution, and if we can find the closed curve which fits into the given boundary shape of the plate and which has the *minimum value of* B/A, then the right-hand side of (1.1)′ provides *a lower bound to the actual collapse pressure*. De Mar (1975), Lin (1977) and Singmaster & Souppouris (1978) have discussed this constrained optimisation problem and given a number of procedures for finding the curve, enclosed in a given convex polygon, which minimizes (B/A). This minimising curve consists of segments of the given boundary joined by circular arcs, all with the *same radius*. Keller (1980) has given an elegant and elementary proof of this result. His paper was motivated by one by Strang (1979), who considered the problem of a long cylinder of plastic material failing in anti-plane shear under a uniform body force. This problem is equivalent to that of a uniformly loaded plastic plate failing by 'punching through' in shear. This problem does not involve bending and is easier and of much less practical interest than that under consideration here.

Lowe (1988*a–c*) and Allen (1992) have investigated a number of cases where upper bound or exact solutions for plate bending problems are known, and have demonstrated that when failure is governed by the square yield condition, the conjecture does hold in every case. Moreover providing the plate is not too elongated, the lower bound approximation given by (1.1) is extremely good. For example for the clamped square plate of side a, (1.1) gives a 'lower bound' of 42.687 for pa^2/M compared with the upper bounds of 42.895 and 42.880 predicted by Mansfield (1957) and Morley (1965) respectively, and the exact value of 42.851 calculated by Fox (1974).

The *strong* conjecture can be given an alternative interpretation. The circular plate which has the same area/perimeter ratio as the given plate mechanism has a radius of $r^* = 2A/B$, an area of $A^* = 4\pi A^2/B^2$ and a perimeter of $B^* = 4\pi A/B$. (Note that $A^* \leqslant A$, with equality only when the original plate is circular.) The collapse pressure associated with this derived circular plate is given by $p/M = 6pk/A^* = (3k/2)(B/A)^2$. Thus whereas the *weak* conjecture states that a given plate is always stronger than the circular plate with the same mechanism area, the *strong* conjecture asserts that it is actually stronger than the *smaller* (and hence stronger) circular plate that has the same area/perimeter ratio as the original mechanism.

The present study is concerned with establishing a proof of the *strong* conjecture (1.1). After reviewing the basic equations of plastic plate theory in §2, the essentially geometric nature of the conjectured inequality is demonstrated in §3. The basic technique used to establish the inequality is the Schwarz Transformation, which is described in §4 and used in §5 to prove the conjecture for the special class of *conical* collapse mechanisms. Pedal coordinates are used to describe the geometry of general mechanisms (§6), which enables a general proof of the conjecture for any mechanism with elliptic or parabolic curvatures to be constructed (§7). The conjecture is hence established for all the familiar solutions obtained from yield line theory. Mechanisms involving regions of hyperbolic curvature are more difficult to analyse. Here, the concept of an angular velocity hodograph diagram is introduced in §8 and a very much weaker and less useful form of the conjecture, which involves the geometry of both the plate mechanism and its hodograph image is discussed in §9 for such anticlastic cases.

2. The basic equations of rigid-plastic plate theory

The quasi-static equilibrium equations for a thin plate in bending are

$$\partial M_{ij}/\partial x_i - Q_j = 0 \quad \text{and} \quad \partial Q_i/\partial x_i + p = 0, \tag{2.1}$$

where M_{ij}, Q_i and p are the cartesian components of the moment tensor, shear force vector and transverse load respectively. Since the present analysis is mainly concerned with properties of upper-bound solutions, little explicit reference will be made to these conditions.

The deformation of the plate at the instant of failure is described by the transverse velocity $v(x_1, x_2)$, which is a continuous though not necessarily continuously differentiable function of position. In developing the theory of rigid-plastic plates it is normal to now define the curvature-rate tensor in terms of the second derivatives of v. However, there are advantages in first introducing the angular velocity of rotation rate vector $\boldsymbol{\omega}$ defined by:

$$\omega_1 = \partial v/\partial x_2, \quad \omega_2 = -\partial v/\partial x_1, \tag{2.2}$$

so that the cartesian components of the curvature-rate tensor can be expressed either by

$$\kappa_{11} = -\partial^2 v/\partial x_1^2, \quad \kappa_{22} = -\partial^2 v/\partial x_2^2, \quad \kappa_{12} = -\partial^2 v/\partial x_1\,\partial x_2, \tag{2.3}$$

or, equivalently, by

$$\kappa_{11} = \frac{\partial \omega_2}{\partial x_1}, \quad \kappa_{22} = -\frac{\partial \omega_1}{\partial x_2}, \quad \kappa_{12} = -\frac{\partial \omega_1}{\partial x_1} = \frac{\partial \omega_2}{\partial x_2}, \tag{2.4}$$

sagging curvatures being taken as positive. The concept of the rotation vector is often used to describe the continuity in slope at a hinge line, but its use as a field variable was introduced by Johnson (1969) and Collins (1971) to explain an analogy between the kinematics of plate and plane strain plasticity problems. From (2.4) we note that $\boldsymbol{\omega}$ is a divergence free vector:

$$\partial\omega_1/\partial x_1 + \partial\omega_2/\partial x_2 = 0. \tag{2.5}$$

In terms of a general orthogonal curvilinear co-ordinate system (α, β) with Lamé parameters h_α, h_β, the components of $\boldsymbol{\omega}$ are

$$\omega_\alpha = \frac{1}{h_\beta}\frac{\partial v}{\partial \beta} \quad \text{and} \quad \omega_\beta = -\frac{1}{h_\alpha}\frac{\partial v}{\partial \alpha} \tag{2.6}$$

and of $\boldsymbol{\kappa}$ are

$$\left.\begin{aligned} \kappa_{\alpha\alpha} &= \frac{1}{h_\alpha}\frac{\partial \omega_\beta}{\partial \alpha} + \frac{\omega_\alpha}{h_\alpha}\frac{\partial \psi}{\partial \alpha}, \quad \kappa_{\beta\beta} = -\frac{1}{h_\beta}\frac{\partial \omega_\alpha}{\partial \beta} + \frac{\omega_\beta}{h_\beta}\frac{\partial \psi}{\partial \beta}, \\ \kappa_{\alpha\beta} &= -\frac{1}{h_\alpha}\frac{\partial \omega_\alpha}{\partial \alpha} + \frac{\omega_\beta}{h_\alpha}\frac{\partial \psi}{\partial \alpha} = \frac{1}{h_\beta}\frac{\partial \omega_\beta}{\partial \beta} + \frac{\omega_\alpha}{h_\beta}\frac{\partial \psi}{\partial \beta}, \end{aligned}\right\} \tag{2.7}$$

PHILOSOPHICAL TRANSACTIONS OF THE ROYAL SOCIETY A MATHEMATICAL, PHYSICAL & ENGINEERING SCIENCES

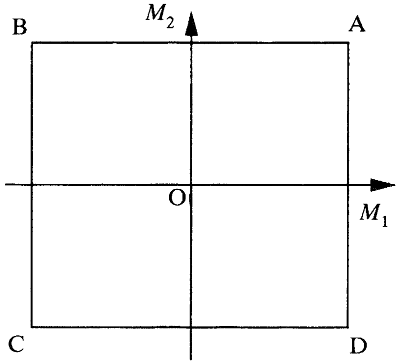

Figure 1. The 'square' yield condition.

where ψ is the anticlockwise inclination of either coordinate line to a fixed reference direction. Eliminating the components of $\boldsymbol{\omega}$ between (2.6) and (2.7) gives the expression for $\boldsymbol{\kappa}$ terms of v as used in Fox (1974).

The contours of constant transverse velocity v will play a central role in the theory. If the curvilinear coordinate system is chosen so that these contours are β-lines, then it follows from (2.6) that $\omega_\alpha = 0$, so that the angular velocity vector is locally tangential to the v-contour. The v-contours are hence also $\boldsymbol{\omega}$-trajectories. The local instantaneous deformation of the plate can be thought of as a rotation, magnitude ω, about the direction of the v-contour.

If (n, s) are now introduced as *local* cartesian coordinates normal and tangential to a v-contour in the level plane, $\boldsymbol{n}$-directed outwards, the angular speed is, using (2.6),

$$\omega = -\partial v/\partial n \tag{2.8}$$

and from (2.7) the corresponding curvature-rate components are

$$\left.\begin{aligned} \kappa_n = \partial\omega/\partial n, \quad \kappa_t = \omega\kappa_s = \omega\,\partial\psi/\partial s, \\ \kappa_{nt} = \partial\omega/\partial s = \omega\,\partial\psi/\partial n, \end{aligned}\right\} \tag{2.9}$$

where $\kappa_s = \partial\psi/\partial s$ is the in-plane curvature of the v-contour. If the v-contour is also a line of principal curvature-rate, the twist rate κ_{nt} is zero and ω is constant along the contour. If such a principal line is a hinge line with a continuously turning tangent then the jump in ω is constant along the hinge (cf. Collins 1971; Fox 1972). It should be emphasized that the components of κ give the instantaneous rates of curvature of the plate as it starts to deform. These components are only the *linear* approximations to the curvature of the three-dimensional surface $z = v(x_1, x_2)$. This fact has to be borne in mind when applying the standard formulae and theorems of the differential geometry of surfaces.

Three basic plastic régimes can be determined for a plate whose collapse is governed by the square yield criterion with associated flow rule. These are typified by the vertex A, sides AB or BC and vertex B of the yield locus (figure 1), where κ_2 has been arbitrarily chosen to be the larger principal curvature rate. Discussions of the governing equations in these régimes have been given by Nielsen (1964, 1984), Massonnet (1967), Sawczuk & Hodge (1968), Fox (1972, 1974) and Collins (1973). For present purposes we recall that at the vertex A, where both principal curvature-rates are non-negative so that the plate is deforming locally into a surface with *elliptical* curvature (positive gaussian curvature), the equilibrium conditions (2.1) can only be satisfied when the transverse load is *zero*. Thus this régime cannot occur in any exact solution for a uniformly loaded plate, except at a single point, such as a vertex in a conical collapse mode. None of the commonly used upper bound mechanisms of yield line theory involve regions in this elliptic régime. If such a mechanism were proposed its associated load-estimate would necessarily be bounded below by that associated with the exact non-elliptic mode.

In an edge régime one of the principal curvature rates is zero, on AB ($\kappa_1 = 0$, $\kappa_2 \geqslant 0$) and on BC ($\kappa_1 \leqslant 0$, $\kappa_2 = 0$), so that the plate is deforming locally into a developable surface with *parabolic* curvature. One of the families of principal curvature trajectories hence consists of straight lines. This considerably simplifies the analysis of both upper bound and exact solutions. Effectively all the collapse mechanisms of yield line theory and all exact solutions, except those for clamped polygonal plates due to Fox (1974), are such that all the deforming regions are in edge régimes. The edge régime BC, with negative parabolic curvature occurs in mechanisms for re-entrant plates. In Fox's solution part of the plate is in the corner régime B, where the principal curvature-rates are of opposite sign. The deformed surface is hence anticlastic with *hyperbolic* curvature. The governing equations are also hyperbolic with many similarities to those for classical slipline theory of plane strain plasticity theory. The curved principal curvature-rate trajectories are the characteristics of both the equilibrium and kinematic equations.

In the present study we are mainly concerned with the analysis of load estimates obtained from upper-bound calculations. These involve equating the rate of working of the uniform applied load distribution to the rate of energy dissipation in the proposed mechanism. In all three of the plastic régimes, this energy dissipation rate per unit area of the plate can be expressed as

$$D \equiv M_{ij}\,\kappa_{ij} = M(|\kappa_1| + |\kappa_2|). \tag{2.10}$$

3. The fundamental inequality

Application of upper bound theorem of limit analysis applied to a uniformly loaded plate, gives the following over-estimate of the collapse pressure:

$$\frac{p}{M} = \left[\int_{A_0} (|\kappa_1| + |\kappa_2|)\,\mathrm{d}A + (k-1)\oint_{C_0} \omega\,\mathrm{d}s\right] \Big/ \int_{A_0} v\,\mathrm{d}A \equiv \frac{W}{V},\ \text{say}, \tag{3.1}$$

where W is the rate of energy dissipation, per unit yield moment, in the mechanism. For a mechanism with a simply supported boundary ($k = 1$) this consists just of the integral of ($|\kappa_1| + |\kappa_2|$), but for a clamped boundary it must include in addition the rate of working on the bounding hinge line. (Note that some well-known upper bound mechanisms for simply supported plates involve corner fans bounded by hinge lines lying within the plate boundary. See for example the solutions given by Mansfield (1957) for triangular plates. The expression for W for such plates must hence include the rate of working on these hinge lines which form just part of the boundary. If these terms are omitted the value of W, and hence of p, is underestimated. Thus if the conjecture can be established for this underestimate of the collapse load it will certainly be true for the actual load associated with such a mechanism. This is the

Table 1. *Integrand of area integral for W – the specific energy dissipation rate in a mechanism* $(\kappa_2 \geqslant 0)$

	simply supported $(k = 1)$	clamped $(k = 2)$
elliptic curvature $(K > 0)$	$\kappa_2 + \kappa_1$	$2(\kappa_2 + \kappa_1)$
hyperbolic curvature $(K < 0)$	$\kappa_2 - \kappa_1$	$2\kappa_2$

approach adopted here.) Since the applied pressure p is uniform, it can be taken outside the integral for the rate of working of the applied loads, as in (3.1) where V denotes the volume of the surface defined by $z = v(x_1, x_2)$.

From (1.1)′ we observe that the conjecture requires

$$(W/V) \geqslant (3k/2)(B/A)^2 \tag{3.2}$$

for all mechanisms. Expressed in this form the required inequality is seen to be a purely *geometric* property of the possible deforming surfaces.

Since the sum of the principal curvature rates (first invariant) is equal to $-\nabla^2 v$ from (2.3) it follows from Green's Theorem that

$$\int_{A_0} (\kappa_t + \kappa_n)\,\mathrm{d}A \equiv \int_{A_0} (\kappa_1 + \kappa_2)\,\mathrm{d}A \equiv \oint_{C_0} \omega\,\mathrm{d}s. \tag{3.3}$$

This is of course a standard result in potential theory. In the present context, however, it is one of a hierarchy of integral identities which relate area integrals to line integrals on v-contours. These need not be discussed at length here, except to note two particular results in passing:

$$\int_{\bar{A}} \kappa_t\,\mathrm{d}A = 2\pi(v_2 - v_1), \tag{3.4}$$

where $\bar{A}$ is the area between the contours C_1, C_2 at depths v_1, v_2 respectively, and

$$\left[\int_0^{2\pi} \omega^2\,\mathrm{d}\psi\right]_{C_1}^{C_2} \equiv \left[\oint \omega\kappa_t\,\mathrm{d}s\right]_{C_1}^{C_2} = 2\int_{\bar{A}} K\,\mathrm{d}A. \tag{3.5}$$

The result (3.4) was used by Schumann (1958*b*), while (3.5) is the linerized form of the Gauss–Bonnet theorem for the area integral of the gaussian curvature rate $K = \kappa_1\kappa_2 = \kappa_t\kappa_n - \kappa_{tn}^2$.

Identity (3.3) can be used to combine the two integrals in the expression for W in (3.1). The results are summarized in table 1 where κ_2 has been arbitrarily chosen to be the non-negative curvature.

In the case of elliptic $(\kappa_1 > 0)$ or parabolic $(\kappa_1 = 0)$ mechanisms, identity (3.3) can alternatively be used to transfer the internal energy dissipation rate to the boundary, so that W can be written as an integral on the boundary contour:

$$W = k\oint_{C_0} \omega\,\mathrm{d}s. \tag{3.6}$$

When the curvature is hyperbolic $(\kappa_1 < 0)$ it follows from table 1 that this equality for W is replaced by a 'greater than' inequality. In many problems the mechanisms will involve internal hinge lines across which the rotation rate is discontinuous and on which one of the curvature rates is infinite. The values of all the above integrals are finite, however, and the identities remain valid provided the contributions from the hinge lines are included in the various area integrals.

The problem of minimizing or finding the stationary values of ratios of integrals as in (3.1) is of course very familiar in applied mathematics. Two well-known examples are

$$\int (\nabla v)^2\,\mathrm{d}A \Big/ \int v^2\,\mathrm{d}A \quad \text{and} \quad \int (\nabla v)^2\,\mathrm{d}A \Big/ \left(\int v\,\mathrm{d}A\right)^2$$

giving the frequencies of a vibrating membrane and the torsional rigidity of an elastic cylinder respectively. The isoperimetric properties of these and similar problems have been extensively studied (see, for example, Pólya & Szegö 1951; Bandle 1980; Schaeffer 1988; Payne 1991). These two particular functionals are quadratic, so that application of the standard techniques of the calculus of variations leads to the familiar linear partial differential equations which characterise the extremal solutions. The functionals in the present problem are specified *piecewise* depending on the sign of the gaussian curvature (cf. table 1). In the elliptic/parabolic region this ratio is $-\int \nabla^2 v\,\mathrm{d}A / \int v\,\mathrm{d}A$ so that both integrals are *linear* and the minimum value must therefore occur at the extremity of this branch, i.e. when $K = 0$ and the mechanism is parabolic. This is an alternative argument demonstrating that exact solutions cannot involve zones with elliptical curvatures. In the hyperbolic régime, however, the integral for W is nonlinear as it involves the *difference* of the principal curvatures and hence introduces the *second* (*quadratic*) invariant of the curvature rate tensor. The minimum value need not now occur at the parabolic limit. For clamped plates it is well known that one frequently cannot obtain exact solutions in which the entire deforming zone is in the parabolic régime. Specifically parabolic fans cannot be continued in a statically admissible manner across a hinge line, as demonstrated by Wood (1969) (see also Collins 1973, or Fox 1974) and such problems require at least part of the deforming zone to be in the hyperbolic régime. The application of the standard calculus of variations argument to the ratio W/V must, of course, yield the equilibrium equations (2.1) as the Euler equation giving sufficient conditions for a minimum.

4. The Schwarz transformation

The Schwarz symmetrization procedure is one of the standard techniques for establishing isoperimetric inequalities (see Pólya & Szegö 1951; Burago & Zalgeller 1980), and as mentioned earlier was used by Schumann (1958*b*) to show that the circular plate is the weakest shaped simply supported plate for a given area. The surface $z = v(x_1, x_2)$ is mapped into an axisymmetric surface, which has the same cross-sectional area at each depth as the original surface (figure 2). Thus each v-contour C of area A is mapped into a circle of radius $(A/\pi)^{\frac{1}{2}}$ and perimeter $(4\pi A)^{\frac{1}{2}}$. The total volume V is preserved by this symmetrization. Schumann then introduces a further transformation in which the symmetrized surface of revolution is replaced by its convex hull, and then demonstrates that under these combined transformations the specific energy dissipation rate W cannot be increased nor V decreased and deduces that $W/V \geqslant 6\pi/A_0$ the collapse load of a circular simply supported plate.

This transformation is now re-examined with a view to establishing the stronger inequality (3.2). If the slope of the original surface normal to the v-contour C_v is

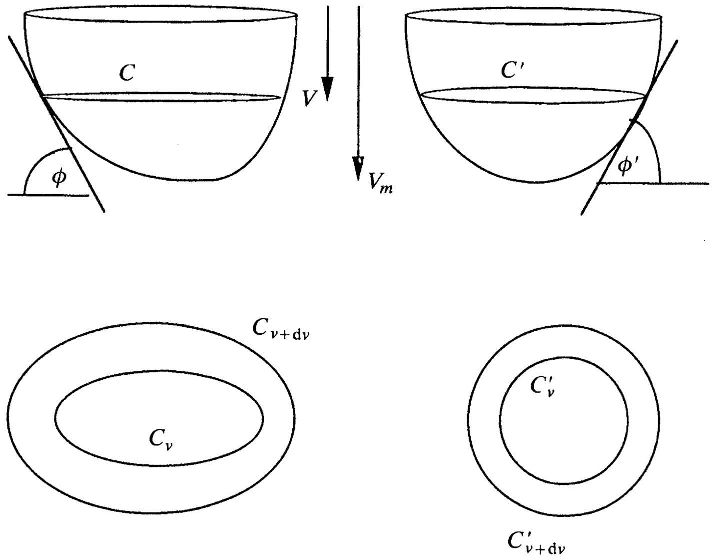

Figure 2. The Schwarz symmetrization.

denoted by ϕ, then $\tan(\phi) = \omega = -\partial v/\partial n$, using (2.8). In general ϕ varies around C_v. The area between the two neighbouring contours C_v and $C_{v+\mathrm{d}v}$ is hence

$$\mathrm{d}A = \oint_{C_v} \mathrm{d}n\,\mathrm{d}s = -\mathrm{d}v \oint_{C_v} \omega^{-1}\,\mathrm{d}s. \tag{4.1}$$

Denoting the *constant* gradient of the image circular contour C'_v on the surface of revolution by $\omega' = \tan(\phi')$, it follows from the basic area preserving property of this symmetrization that this elemental area is also given by

$$\mathrm{d}A = -\mathrm{d}v \oint_{C'_v} \omega'^{-1}\,\mathrm{d}s' = -\mathrm{d}v\omega'^{-1}(4\pi A)^{\frac{1}{2}} \tag{4.2}$$

so that

$$\omega' = (4\pi A)^{\frac{1}{2}} \Big/ \oint_{C_v} \omega^{-1}\,\mathrm{d}s = -(4\pi A)^{\frac{1}{2}} \frac{\mathrm{d}v}{\mathrm{d}A}. \tag{4.3}$$

Now it follows from the fundamental Schwarz integral inequality that

$$\oint_C \omega\,\mathrm{d}s \geqslant B^2 \Big/ \oint_C \omega^{-1}\,\mathrm{d}s \tag{4.4}$$

for any contour C. Hence applying (4.3) and (4.4) to the boundary contour C_0 we deduce that

$$\frac{1}{V}\int_{C_0} \omega\,\mathrm{d}s \geqslant \frac{3}{2}\frac{B_0^2}{A_0^2}\frac{V_c}{V}, \tag{4.5}$$

where $V_c = \frac{1}{3}\omega'_0(A_0^3/\pi)^{\frac{1}{2}}$ is the volume of the circular cone with A_0 as base and slope ω'_0. Hence it follows from (3.2), (3.6) and (4.5) that a *sufficient* condition for the conjecture to hold is that $V \leqslant V_c$. This is true in particular when the symmetrical surface of revolution lies everywhere within this cone (figure 2). This condition will be returned to in the following.

For future reference we will note the expressions for the curvatures of the symmetrized surface of revolution. If a is the radius of the circular cross section at

PHILOSOPHICAL TRANSACTIONS OF THE ROYAL SOCIETY A MATHEMATICAL, PHYSICAL & ENGINEERING SCIENCES

depth v, the components of the curvature rate tensor associated with the symmetrized surface of revolution are:

$$\left.\begin{aligned} \kappa_2' \equiv \kappa_t' &= \frac{\omega'}{a} = -\frac{1}{a}\frac{\mathrm{d}v}{\mathrm{d}a}, \quad \kappa_1' \equiv \kappa_n' = \frac{\mathrm{d}\omega'}{\mathrm{d}a} = -\frac{\mathrm{d}^2 v}{\mathrm{d}a^2}, \\ K' &= \kappa_1' \kappa_2' = \frac{\omega'}{a}\frac{\mathrm{d}\omega'}{\mathrm{d}a} = \frac{1}{a}\frac{\mathrm{d}v}{\mathrm{d}a}\frac{\mathrm{d}^2 v}{\mathrm{d}a^2} = \pi\frac{\mathrm{d}(\omega'^2)}{\mathrm{d}A}. \end{aligned}\right\} \tag{4.6}$$

As remarked earlier these are the linearized curvatures of the actual surface; the exact curvatures are obtained by dividing the three expressions in (4.6) by $\gamma^{\frac{1}{2}}$, $\gamma^{\frac{3}{2}}$ and γ^2 respectively, where $\gamma = (1+\omega'^2)$.

From (4.3) it follows that these curvature rate components are related to the corresponding components in the actual deformation by

$$2\pi\kappa_t'^{-1} = \int_0^{2\pi} \kappa_t^{-1}\,\mathrm{d}\psi \equiv \oint_C \omega^{-1}\,\mathrm{d}s = -\frac{\mathrm{d}A}{\mathrm{d}v} \tag{4.7}$$

so that κ_t' is the reciprocal mean tangential curvature rate. Similarly the corresponding normal curvature rate is seen to be

$$\kappa_n' = -2\pi\frac{\mathrm{d}}{\mathrm{d}v}\left[A\left(\oint_C \omega^{-1}\,\mathrm{d}s\right)^{-2}\right] = -2\pi\frac{\mathrm{d}}{\mathrm{d}v}\left[A\left(\frac{\mathrm{d}A}{\mathrm{d}v}\right)^{-2}\right], \tag{4.8}$$

while the gaussian curvature rate can be expressed:

$$K' = \pi\frac{\mathrm{d}(\omega'^2)}{\mathrm{d}A} = 4\pi^2\left(\frac{\mathrm{d}A}{\mathrm{d}v}\right)^{-4}\left[\left(\frac{\mathrm{d}A}{\mathrm{d}v}\right)^2 - 2A\frac{\mathrm{d}^2 A}{\mathrm{d}v^2}\right]. \tag{4.9}$$

The Schwarz symmetrization can be regarded as a geometrical visualization of the A–v relation in the original mechanism. In particular we note that the solution to the differential equation obtained by putting $K' = 0$ in (4.9) describes the cone:

$$A = A_0(1 - v/v_m)^2. \tag{4.10}$$

This occurs when the original mechanism is conical, but with an arbitrarily shaped initial cross section with area A_0. This case is discussed in §5.

The interpretation of the *strong* conjecture in terms of a reduced circular plate given in §1 suggests an alternative possible transformation, in which the *ratio* of the area to the perimeter instead of the area itself is preserved. To preserve the total 'volume' of the mechanism the transverse velocity field v must also be scaled. The radius of an image circular contour C^* is now $r^* = 2A/B$, its area is $A^* = 4\pi A^2/B^2$ and its perimeter is $B^* = 4\pi A/B$, whilst the increment in velocity between neighbouring contours becomes $\mathrm{d}v^* = (B^2/4\pi A)\,\mathrm{d}v$. If the constant gradient of the image surface at the image contour C^* is denoted by $\omega^* = \tan(\phi^*)$, the increment in A^*/B^* between two neighbouring contours with separation $\mathrm{d}v^*$ is found to be:

$$\mathrm{d}(A^*/B^*) = -\mathrm{d}v^*/2\omega^*. \tag{4.11}$$

On the other hand the corresponding relation in the original mechanism is

$$\begin{aligned} \mathrm{d}(A/B) &= (\mathrm{d}A - A\,\mathrm{d}B/B)/B \\ &= -\frac{\mathrm{d}v}{B}\left[\oint_C \omega^{-1}(1-(A/B)\,\kappa_t\,\omega^{-1})\,\mathrm{d}s\right], \end{aligned} \tag{4.12}$$

where (4.1) has been used to eliminate $\mathrm{d}A/\mathrm{d}v$, and the corresponding relation:

$$\mathrm{d}B = -\mathrm{d}v \oint_C \omega^{-2}\kappa_t \,\mathrm{d}s = -\mathrm{d}v \int_0^{2\pi} \omega^{-1}\,\mathrm{d}\psi \tag{4.13}$$

used to eliminate $\mathrm{d}B/\mathrm{d}v$. Equating the two left-hand sides of (4.11) and (4.12) gives the relation between ω and ω^* analogous to (4.3) for the Schwarz transformation:

$$\omega^{*-1} = \frac{8\pi A}{B^3}\left\{\oint_C \omega^{-1}\,\mathrm{d}s - \frac{A}{B}\int_0^{2\pi} \omega^{-1}\,\mathrm{d}\psi\right\}. \tag{4.14}$$

Since the *strong* conjecture can be expressed in terms of a direct comparison between the failure pressures of the original and the derived circular plate mechanisms, this transformation offers the possibility of establishing the conjecture, by using (4.14) to compare the specific energy dissipation rates, W and W^*, in the two mechanisms. W is given by (3.1) or (3.6), and W^* is found from analogous expressions involving the derived velocity field v^*, which is now *viewed as defining a collapse mechanism* for the circular plate. The upper bound theorem of limit analysis could then be invoked to compare W^* with the energy dissipation rate and hence the known collapse pressure in the *actual* circular plate collapse mechanism. This is essentially the approach adopted by Schumann (1958*b*) in using the Schwarz transformation to establish the *weak* conjecture. However, the extra complexity of (4.14) compared with (4.3) for the Schwarz transformation has, so far, prevented much general progress being made with this line of attack on the *strong* conjecture. It seems necessary to consider the collapse mechanism in more detail as is done in the following sections.

5. Conical mechanisms

Before discussing general classes of mechanisms it is instructive to consider the special case of a simply supported plate collapsing into a conical surface with vertex at some point 0 say. The plate boundary need not be convex. Many such examples have been discussed in the literature (e.g. Mansfield 1957; Wood 1961; Massonnet 1967; Sawczuk & Jaeger 1963). The mechanism boundaries may contain straight segments, in which case the mechanism contains rigid flaps rotating about such straight edges, and corners in which case the mechanism contains internal hinge lines as in figure 3.

If $r = r_0(\theta)$ is the polar equation of the boundary contour referred to 0 and v_m is the transverse velocity at the vertex 0, the velocity at an arbitrary point distant r from 0 is

$$v = v_m(1 - r/r_0). \tag{5.1}$$

The v-contours are hence geometrically similar to the boundary contour, and the area of a typical contour is given by (4.10). Since each radial segment of the plate OP rotates with angular speed ω about the tangent to the boundary at P, the transverse speed at the origin is

$$v_m = p_0\,\omega, \tag{5.2}$$

where $p_0 = ON$ is the *pedal* coordinate of P, the perpendicular distance from the origin to the tangent to C_0 at P. Pedal coordinates are hence seen to arise naturally in describing the kinematics of collapse mechanisms. They also arise naturally in the

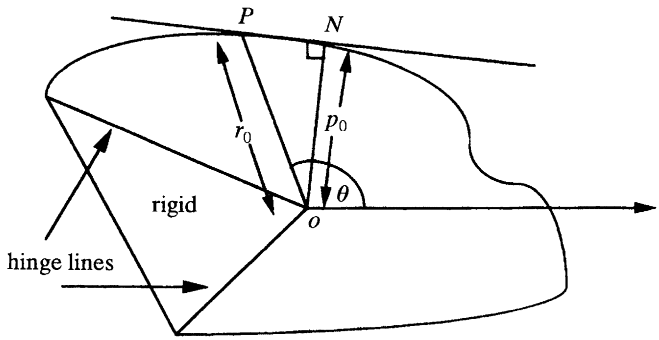

Figure 3. A conical collapse mechanism.

discussion of the classical isoperimetric inequality and indeed were used in the first analytical proof of the result due to Hurwitz (1902) (see Hsiung 1981). This is because the area enclosed by a closed plane curve C is given by half the line integral of p:

$$2A = \oint_C p \, \mathrm{d}s. \tag{5.3}$$

It has already been shown in equation (3.6) that the energy dissipation rate for a parabolic mechanism in a simply supported plate can be transferred to the boundary and expressed as

$$W = \oint_{C_0} \omega \, \mathrm{d}s = v_m \oint_{C_0} p_0^{-1} \, \mathrm{d}s \tag{5.4}$$

using (5.2). But from (5.3) and the Schwarz inequality we obtain:

$$\oint_{C_0} p_0^{-1} \, \mathrm{d}s \geqslant \left(\oint_{C_0} \mathrm{d}s \right)^2 \Big/ \oint_{C_0} p_0 \, \mathrm{d}s = B_0^2/2A_0. \tag{5.5}$$

Moreover since the volume of any conical collapse mechanism is simply $\frac{1}{3}A_0 v_m$ it follows that from (5.4) and (5.5) that

$$W/V \geqslant 3B_0^2/2A_0^2. \tag{3.2}$$

The conjecture has hence been proved for any conical collapse mode. The extension to clamped plates follows trivially by doubling the expression for W in (5.4). This proof is essentially that given by Allen (1992).

The right-hand side of this inequality is of course independent of the position of the vertex 0 inside C_0. The best upper bound mechanism is obtained by choosing 0 to minimize the value of $\oint p_0^{-1} \mathrm{d}s$. Equality is obtained in (3.2) only when the Schwarz inequality also reduces to an equality. This requires p to be a constant, which at first sight would appear to imply that C_0 must be a circle. However, when C_0 is a polygon, ds is zero at the vertices and contributes nothing to the line integral. Thus equality is also obtained in (3.2) when C_0 is a polygon which possesses an inscribed circle which touches every side, and the vertex is chosen to be the centre of this circle. For such plates the value of B/A is the same for the plate as it is for the incircle (Allen 1992) and the corresponding pyramidal mechanism has constant slope as discussed by Lowe (1982). Several such solutions have been discussed by Sawczuk & Jaeger (1963).

One reason for the simplicity of the analysis in this case is the simple quadratic form of the A–v relation (4.10) for a conical collapse mode. In fact this relation is quadratic for *any* parabolic mechanism, i.e. any mechanism consisting of rigid rotating flaps and plastically deforming regions which are in an edge régime on the yield surface. A formal proof of this result is given in §7 once the mathematics for describing the kinematics of the deformation has been set up in the next Section. However, a preliminary argument justifying this quadratic variation can be given now.

Since one of the principal curvature rates is zero in a parabolic region one family of principal curvature trajectories consists of straight lines. A rigid rotating region, bounded by such a *straight* principal line, is locally trapezoidal so that the local A–v relation in such a region is clearly quadratic. Within a deforming zone the twist rate is zero along a principal curvature rate line; if in addition this line (an α-line say) is straight, as in such a parabolic region, ω_α the component of the angular velocity vector in the directioin of this line must be constant along this α-line (cf. equation (2.7)). Moreover since the associated curvature rate is zero, ω_β the component of angular velocity perpendicular to this line, is also invariant along the α-line. It follows that the *total angular velocity vector* is similarly constant. The v-contours in a parabolic region are hence parallel curves and corresponding points are rotating at the same speed. The speed v hence varies linearly along the straight principal line which again implies a quadratic A–v relation.

If this quadratic relation is written:

$$A = a + bv + cv^2, \tag{5.6}$$

then the (linearized) gaussian curvature of the symmetrized image is, using (4.9),

$$K' = 4\pi^2(b^2 - 4ac)/(b + 2cv)^4. \tag{5.7}$$

When the discriminant $D = (b^2 - 4ac)$ is positive or zero, this curvature is elliptic or parabolic and the symmetrized image surface of revolution lies inside, or coincides with, the base tangent cone, and the strong conjecture is proven as discussed in §4. $D \geqslant 0$ is, of course, the condition for the equation $A = 0$ to have real roots. This must be the case as the mechanism must terminate in a ridge or point vertex of zero area. This provides a proof of the conjecture in the case of a 'single mode' mechanism in which the A–v relation is represented by a *single* quadratic expression. It will be seen in §8 however that when the mechanism contains 'floating fans' with vertices which do not coincide with the mechanism vertex, the A–v relation is only piecewise quadratic and further considerations are necessary.

6. The geometry of v-contours

As a result of the successful use of pedal coordinates in establishing the conjecture for conical mechanisms, it is natural to use pedal or tangential coordinates (p, ψ) to describe the geometry of v-contours in the general case. In this section discussion is limited to mechanisms with weakly convex contours, so that ψ, the inclination of the tangent to a contour, increases monotonically from 0 to 2π. The theory of curves expressed in terms of such coordinates can be found in classical elementary calculus texts such as Courant & John (1974) (see also Hsuing 1981). For present purposes we recall that the distance from P to the foot N of the perpendicular from 0 to the

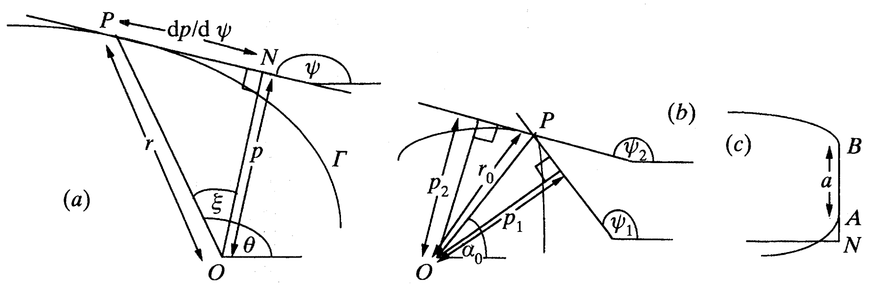

Figure 4. Pedal representation of contours including corners and flats.

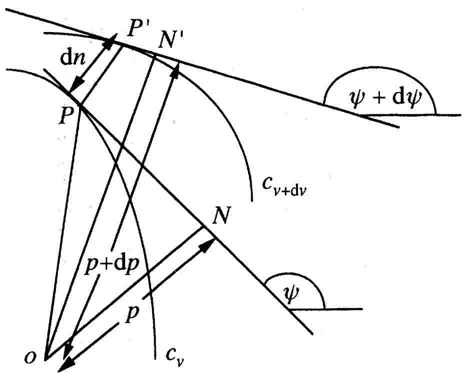

Figure 5. Two neighbouring contours.

tangent to Γ at P is $\mathrm{d}p/\mathrm{d}\psi$ (figure 4*a*), and that the radius of curvature of Γ at P is $p+\mathrm{d}^2p/\mathrm{d}\psi^2$. The angle between the radial and tangential directions at P is $\frac{1}{2}\pi-\xi$, where

$$\tan\xi = r^{-1}\,\mathrm{d}r/\mathrm{d}\theta = p^{-1}\,\mathrm{d}p/\mathrm{d}\psi, \quad \cos\xi = p/r, \quad \text{and } \psi = \theta+\tfrac{1}{2}\pi-\xi. \tag{6.1}$$

The v-contours of the collapsing plate mechanisms are frequently not smooth but contain corners and straight segments. Our mathematical description of the contours must be able to handle such features. At a corner ψ is discontinuous, increasing from ψ_1 to ψ_2 say (figure 4*b*) and the radius of curvature vanishes so that $p(\psi)$ is a harmonic function in the interval (ψ_1, ψ_2) and is given by

$$p = r_0\cos(\psi-\alpha_0-\tfrac{1}{2}\pi) \text{ or } = (p_1\sin(\psi_2-\psi)+p_2\sin(\psi-\psi_1))/\sin(\psi_2-\psi_1). \tag{6.2}$$

On a straight segment of the contour, ψ and p are constant, but $\mathrm{d}p/\mathrm{d}\psi$ is discontinuous, its value increasing by the length a of the straight segment (figure 4*c*) and hence $\mathrm{d}^2p/\mathrm{d}\psi^2 = a\delta(\psi-\psi_0)$. It follows that weakly convex contours with corners can be represented by a continuous function $p(\psi)$ and the standard formulae for radius of curvature, arc length and area still apply, but the former has a delta function behaviour on a flat portion of the contour.

The family of contours on a plate can be parametrized by $p = p(\psi, v)$, the origin being chosen to be one of the points where v attains its maximum value. The normal distance between two neighbouring contours C_v and $C_{v+\mathrm{d}v}$ is $\mathrm{d}n = -\omega^{-1}\,\mathrm{d}v$ (cf. (4.1)) (figure 5). Since the difference between $\mathrm{d}n$ and $\mathrm{d}p$ is second order this result can also be written:

$$\partial p/\partial v = -\omega^{-1}. \tag{6.3}$$

This important relation expresses the fundamental kinetic result that as a plate element is rotating with angular speed ω, the change in the transverse velocity in going a distance $\mathrm{d}p$ normal to the axis of rotation is $\omega\,\mathrm{d}p$.

The second basic result needed is an expression for $\partial\omega/\partial v$. Since PN is of length $\partial p/\partial\psi$, the length of $P'N'$ is

$$\partial p/\partial\psi + (\partial^2 p/\partial\psi^2)\,\mathrm{d}\psi + (\partial^2 p/\partial\psi\,\partial v)\,\mathrm{d}v,$$

where $\mathrm{d}\psi$ is the change in the slope of the tangents between P and P'. But $P'N'$ is also the projection of $\overrightarrow{ON}+\overrightarrow{NP}$ onto the tangent at P', and hence is equal to $-p\,\mathrm{d}\psi + \partial p/\partial\psi$, from which we deduce that

$$\mathrm{d}\psi = ((-\partial^2 p/\mathrm{d}\psi\,\partial v)/(p+\partial^2 p/\partial\psi^2))\,\mathrm{d}v. \tag{6.4}$$

It follows from (2.9) that

$$\partial\omega/\partial\psi = \omega\kappa_{nt}/\kappa_t \tag{6.5}$$

so that from (6.3) $\partial^2 p/\partial\psi\,\partial v = \omega^{-1}\kappa_{nt}/\kappa_t$, and since $p+\partial^2 p/\partial\psi^2 = \omega\kappa_t^{-1}$ we can rewrite (6.4) as

$$\mathrm{d}\psi = -\omega^{-2}\kappa_{nt}\,\mathrm{d}v. \tag{6.4$'$}$$

The change in the angular speed between P and P' is therefore:

$$\mathrm{d}\omega = \frac{\partial\omega}{\partial\psi}\mathrm{d}\psi + \frac{\partial\omega}{\partial v}\mathrm{d}v = \left(-\omega^{-1}\frac{\kappa_{nt}^2}{\kappa_t} + \frac{\partial\omega}{\partial v}\right)\mathrm{d}v. \tag{6.6}$$

However, since from (2.8) and (2.9) we also have $\mathrm{d}\omega = \partial\omega/\partial n\,\mathrm{d}n = -\omega^{-1}\kappa_n\,\mathrm{d}v$ we deduce the second important kinematic result that

$$\partial\omega/\partial v = -\omega^{-1}K/\kappa_t, \tag{6.7}$$

where K is the gaussian curvature rate. It follows that in a parabolic region where the gaussian curvature rate vanishes, ω is a function of ψ only and is the same for all contours. This is a formal proof of the result discussed at the end of §5. This proof breaks down at a fan vertex where the curvature rates are unbounded. This situation is discussed in §8.

7. Parabolic mechanisms

In this section we use the formalism of §6 to generalize the proof given in §5 for conical collapse mechanisms, to arbitrary parabolic mechanisms consisting of weakly convex contours. The origin 0 of the pedal coordinate system is chosen to be any point where v attains its maximum value v_{m}, such as the mid-point of a straight ridge. The pedal equation of the ridge contour C_1 will be denoted by $p = p_1(\psi)$. (For example the straight ridge $(-a \leqslant x \leqslant a)$ has pedal equation $p_1 = a|\sin\psi|$, the jumps in the value of $\mathrm{d}p/\mathrm{d}\psi$ occurring at $\psi = 0$ and π correspond to the two coincident straight edges of the ridge.) As previously noted when the gaussian curvature rate is zero and the mechanism does not contain any floating fans, ω is independent of v and equation (6.3) integrates to give

$$p(\psi, v) = p_0(\psi) - \omega^{-1}(\psi)\,v, \tag{7.1}$$

where $p_0(\psi)$ is the pedal equation of the boundary contour, $v = 0$. Hence putting $v = v_{\mathrm{m}}$:

$$v_{\mathrm{m}}\,\omega^{-1}(\psi) = p_0(\psi) - p_1(\psi) \tag{7.2}$$

and so eliminating ω, we obtain the pedal equation of a general contour:

$$p(\psi, v) = (1-v/v_{\mathrm{m}})\, p_0(\psi) + (v/v_{\mathrm{m}})\, p_1(\psi). \tag{7.3}$$

The lower bound on the energy dissipation rate obtained from the Schwarz inequality is

$$\oint_{C_0} \omega \,\mathrm{d}s_0 \geqslant B_0^2 \Big/ \oint_{C_0} \omega^{-1}\,\mathrm{d}s_0 = v_m B_0^2/2(A_0 - \tfrac{1}{2}I_0) \tag{7.4}$$

using (7.2) to evaluate the integral of ω^{-1}, where the integral I_0 is defined by

$$I_0 = \oint_{C_0} p_1 \,\mathrm{d}s_0. \tag{7.5}$$

It follows from (7.3) that the elemental arc lengths on C, C_0 and C_1 are related by

$$\mathrm{d}s = (1-v/v_{\mathrm{m}})\,\mathrm{d}s_0 + (v/v_{\mathrm{m}})\,\mathrm{d}s_1 \tag{7.6}$$

so that the area enclosed by an arbitrary contour C is A where

$$2A = \oint_C p\,\mathrm{d}s = 2\left(1-\frac{v}{v_{\mathrm{m}}}\right)^2 A_0 + \left(\frac{v}{v_{\mathrm{m}}}\right)\left(1-\frac{v}{v_{\mathrm{m}}}\right)(I_0 + I_1) \tag{7.7}$$

using (7.3) and (7.6). The integral I_1 is in fact identical with I_0 since

$$I_1 = \oint p_0\,\mathrm{d}s_1 = \int_0^{2\pi} p_0(p_1 + p_1'')\,\mathrm{d}\psi = \int_0^{2\pi} p_1(p_0 + p_0'')\,\mathrm{d}\psi = I_0. \tag{7.8}$$

The equality of the two ψ integrals follows by integration by parts or by expanding p_0, p_1 as Fourier series. The latter procedure is more general as it includes the case of contours with flats where the second derivative of the pedal-coordinate has a δ-function singularity.

The total 'volume' of the mechanism is, using (7.7),

$$V = \int_0^{v_{\mathrm{m}}} A\,\mathrm{d}v = \tfrac{1}{3}v_{\mathrm{m}}(A_0 + \tfrac{1}{2}I_0). \tag{7.9}$$

The required inequality now follows from (7.4) and (7.9)

$$\frac{1}{V}\oint_{C_0} \omega\,\mathrm{d}s \geqslant \frac{3}{2}\frac{B_0^2}{(A_0^2 - \frac{1}{4}I_0^2)} \geqslant \frac{3}{2}\frac{B_0^2}{A_0^2}. \tag{7.10}$$

The quadratic A–v relation is given explicitly in (7.7) with discriminant $D = I_0 v_{\mathrm{m}}^{-2}$, so that the symmetrical surface is parabolic (i.e. a cone) when $I_0 = 0$ and the mechanism has a focus, as already shown in §5, but is elliptic when $I_0 > 0$ as when the mechanism has a ridge. The elliptic curvature guarantees that the symmetrized surface lies within the tangent cone on A_0, so that the sufficient conditions for the conjecture to hold discussed in §4 hold for all such parabolic mechanisms.

When the mechanism does involve floating fans, the curvature is unbounded at the fan vertex, and the A–v relation is only piecewise quadratic. However, the sign of the jump across the contour through such a vertex is such as to ensure that the symmetrized surface still lies inside the base tangent cone. This case is best discussed with reference to the hodograph diagram and is returned to at the end of the next section.

The above proof is readily extended to non-convex plates, such as the L-shaped plates considered by Jones & Wood (1967). The quadratic A–v relation can be seen either by applying the (p, ψ) parametrization piecewise over segments on which ψ is monotonic, or by appealing to the 'local' argument used at the end of §5. Parabolic mechanisms for such re-entrant plates will in general involve regions in which the plate is in edge régime BC as well as AC (figure 1). The equality in (3.6) must now be replaced by a 'greater than' inequality. The above proof of the conjecture hence still holds but the lower bounds it provides will, in general, be less sharp than for a convex plate (Allen 1992).

8. The hodograph diagram

The hodograph or velocity diagram although widely used in plane strain plasticity theory is rarely used in plate problems. It is, however, a useful geometrical aid in discussing the kinematics of collapse mechanisms, particularly the more complicated ones in which both families of principal lines are curved. Some examples of plate hodographs are given in the papers by Johnson (1969) and Collins (1971). The image of any point P in the plate is the point Q in the hodograph diagram with position vector $\boldsymbol{\omega}$. The hodograph image of a contour C_v whose pedal equation is $p = p(\psi, v)$ is C'_v whose *polar* equation is $\omega = \omega(\psi, v)$. The radius vector at Q is hence in the direction of the tangent vector to C_v at P.

If the angle between the radius vector and the normal to the hodograph image contour is $\frac{1}{2}\pi - \eta$, then $\chi = \psi + \frac{1}{2}\pi - \eta$ is the slope of the tangent vector and by analogy with (6.1):

$$\tan\eta = \frac{1}{\omega}\frac{\mathrm{d}\omega}{\mathrm{d}\psi} = \frac{\kappa_{nt}}{\kappa_t} = \frac{1}{q}\frac{\mathrm{d}q}{\mathrm{d}\chi} \quad \text{and} \quad \cos\eta = \frac{q}{\omega}, \tag{8.1}$$

where q is the pedal-coordinate of the hodograph diagram (figure 6) and use has been made of (6.5). The length of a hodograph image contour is hence

$$B_\mathrm{h} = \oint_{C'_v} \mathrm{d}\sigma = \oint_{C'_v} \surd(\kappa_{nt}^2 + \kappa_t^2)\,\mathrm{d}s, \tag{8.2}$$

while its enclosed area is

$$A_\mathrm{h} = \frac{1}{2}\oint_{C_v} \omega^2\,\mathrm{d}\psi. \tag{8.3}$$

The fundamental integral identity (3.5) shows that the area between two hodograph image contours is equal to the integral of the gaussian curvature-rate over the corresponding annular region between the two original v-contours. If the curvature rate is parabolic it follows that all the hodograph images must coincide as discussed above. In a hyperbolic region, however, K is negative and the v-contours and their hodograph images must nest in opposite senses.

In the special case of the conical collapse modes $\omega p = v_\mathrm{m}$, from which it follows from (6.1) and (8.1) that

$$\eta = -\xi \quad \text{and} \quad rq = \omega p = v_\mathrm{m} \tag{8.4}$$

so that the hodograph image curve is the pedal inverse of a plate boundary contour

Figure 6

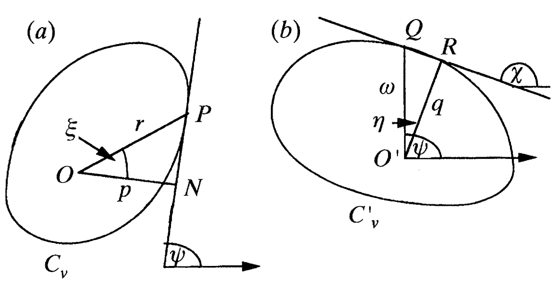

Figure 7

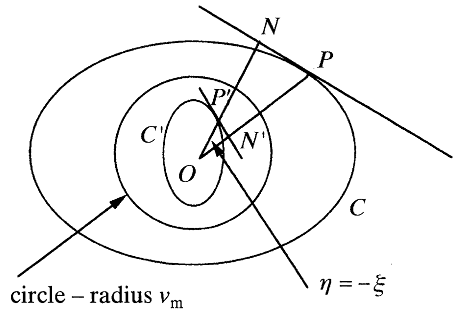

Figure 6. The hodograph transformation: (*a*) physical plane of plate; (*b*) hodographic plane.
Figure 7. In a conical collapse mode the hodograph image is the pedal inverse in circle of radius v_{m}.

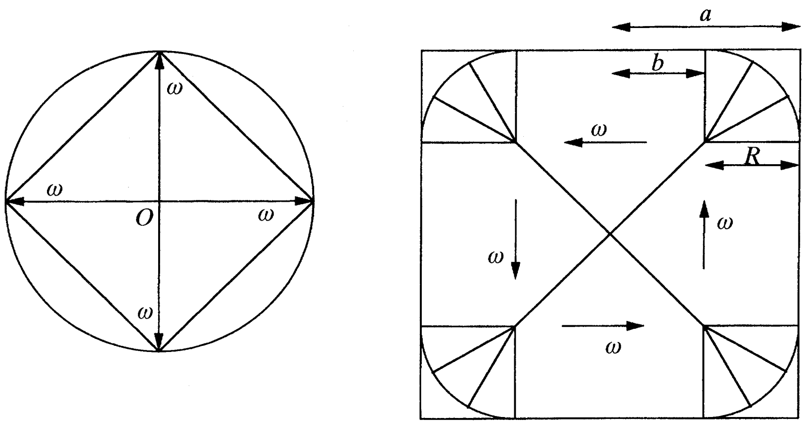

Figure 8. Wood's (1961) hodograph and collapse mechanism for a clamped square plate.

in the circle of radius v_{m}, see figure 7. For the generalization to follow it is relevant to note that as a consequence of (8.4), the expression for the energy dissipation rate in (5.4) can also be written as a line integral in the hodograph diagram:

$$\oint_{C_0} \omega \, \mathrm{d}s = v_{\mathrm{m}} \oint_{C'_0} \frac{\mathrm{d}\sigma}{q}. \tag{8.5}$$

On a straight section of a contour, the direction of $\boldsymbol{\omega}$ is constant. If this section is also a principal curvature line, as it must be of necessity in a parabolic mode, its hodograph image is a point. In a hyperbolic mode, however, such a section will be represented by straight spike locally normal to the hodograph curve.

The hodograph diagram for Wood's mechanism for a square, clamped plate is shown in figure 8. The four rigidly rotating flaps are represented by the four mutually orthogonal $\boldsymbol{\omega}$ vectors. In the outer part of the mechanism the rotation in the fans is represented in the hodograph by the four 90° circular arcs. In contrast in the inner section, where the flaps are separated by straight hinge lines, the transition from one $\boldsymbol{\omega}$ vector to the next is achieved by a discontinuous jump. In such mechanisms therefore the hodograph image is not really a single curve as argued above. This situation arises in all parabolic mechanisms involving floating fans. The curvature rates are necessarily unbounded at the vertex of such a fan.

The area–velocity relationship for this mechanism is only piecewise parabolic. In the outer region ($v \leqslant v_1 = \omega R = v_m(R/a)$) this relation is

$$A = 4b^2 + 8b(R - a(v/v_m)) + \pi(R - a(v/v_m))^2, \tag{8.6}$$

while in the inner region it is

$$A = 4a^2(1-(v/v_m))^2. \tag{8.7}$$

A and dA/dv are continuous at the transition contour $v = v_1$, but the value of $d^2A/dv^2 = 2c$ in (5.6) *decreases* from $8\omega_0^{-2}$ and $2\pi\omega_0^{-2}$ in crossing from the inner to the outer section of the mechanism. It follows that the value of the symmetrized gaussian curvature K' defined in (5.7) is greater in the outer region than it is in the inner one. The argument used in §5 to show that K' is positive still applies to the inner section since this contains the apex where $A = 0$. K' is hence positive throughout the entire plate. The sign of the jump in the second derivative of A with respect to v will always be of this sign in any mechanism containing an internal fan vertex, as can be seen from the hodograph image. The contribution to d^2A/dv^2 from a fan or hinge is $\int \omega^{-2}\,d\psi$, which is twice the area of the polar segment of the inverse of the hodograph image curve in the unit circle. This area is always greater for the hinge than for a fan since the magnitude of ω is larger in the fan than in the hinge. The proof of the conjecture hence carries over to such piecewise parabolic mechanisms.

9. Parabolic–hyperbolic mechanisms

The problem of generalizing the above argument to include mechanisms with hyperbolic régimes, such as Fox's clamped square plate solution does not appear to be straightforward. Firstly since the gaussian curvature is now merely one signed rather than zero the equalities deduced in §7 are now replaced by inequalities. In addition as already noted the internal energy dissipation rate W is now a *nonlinear* functional of the curvature rates, involving the *difference* of the principal curvature rates. Although W is still bounded below by the boundary integral (3.6), this proves too weak a bound to prove the conjecture. Here we restrict attention to centred mechanisms with convex contours and show that the 'natural' generalization of the above argument leads to an isoperimetric inequality which involves the geometry of the *hodograph* diagram as well as that of the plate.

When the gaussian curvature rate K is non-positive it follows from (6.7) that $\partial^2 p/dv^2$ is non-negative everywhere, provided $\kappa_t \geqslant 0$, so that the v-contours are weakly convex. Thus from (6.3) and the mean value theorem it follows that

$$-\omega^{-1}(\psi, v_2) \geqslant (p(\psi, v_2) - p(\psi, v_1))/(v_2 - v_1) \geqslant -\omega^{-1}(\psi, v_1), \tag{9.1}$$

where $0 \leqslant v_1 \leqslant v_2 \leqslant v_m$, with equality only when $K = 0$. In particular putting $v_1 = 0$, $v_2 = v_m$ and assuming a single vertex mechanism, it follows that on the boundary contour C_0:

$$\omega_0(\psi) \leqslant v_m/p_0(\psi). \tag{9.2}$$

Comparison with (5.4) and (5.5) shows that this inequality is of the wrong sign for the desired lower bound on the specific energy dissipation rate W to be established. For modes including hyperbolic regimes therefore a stronger inequality than (3.6) is needed for W.

PHILOSOPHICAL TRANSACTIONS OF THE ROYAL SOCIETY A MATHEMATICAL, PHYSICAL & ENGINEERING SCIENCES

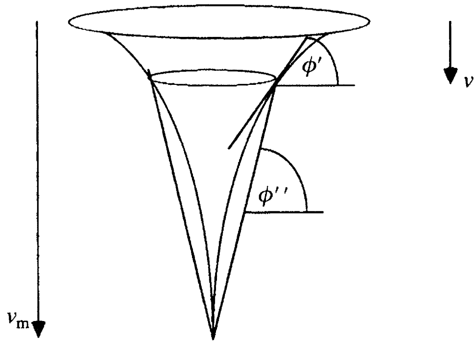

Figure 9. Schwarz symmetrization for hyperbolic/parabolic mechanisms.

Putting $v_1 = v$, $v_2 = v_m$ in (9.1) yields the further inequality:

$$\omega^{-1}(\psi, v) \geqslant p(\psi, v)/(v_m - v) \tag{9.3}$$

so that

$$\oint_C \omega^{-1}\,ds \geqslant 2A/(v_m - v). \tag{9.4}$$

From (4.3) and (9.4), the gradient of the transformed symmetrical image surface of revolution satisfies

$$\tan(\phi') \equiv \omega' \leqslant (v_m - v)/(A/\pi)^{\frac{1}{2}} \equiv \tan(\phi''), \tag{9.5}$$

where ϕ'' is the slope of the circular cone with base C' and vertex at v_m (see figure 9). The symmetrized surface of revolution hence also has parabolic–hyperbolic curvature, so that its total volume cannot exceed $\frac{1}{3}A_0 v_m$. In contrast to (9.2) this inequality is of the correct sign to give a lower bound on the estimated collapse pressure.

To obtain a sharper inequality for the energy dissipation rate we recall that the exact expressions for W for clamped and simply supported plates are given in table 1. The energy dissipation rate per unit area is $(\kappa_2 - \kappa_1)$ for a simply supported plate and $2\kappa_2$ for a clamped plate. Thus in terms of the two invariants, the mean and gaussian curvatures rates,

$$H = \tfrac{1}{2}(\kappa_1 + \kappa_2) = \tfrac{1}{2}(\kappa_t + \kappa_n) \quad \text{and} \quad K = \kappa_1\kappa_2 = \kappa_t\kappa_n - \kappa_{tn}^2 \tag{9.6/9.7}$$

the energy dissipation rate in the mechanism can be written:

$$W = \int 2((H^2 - K)^{\frac{1}{2}} + (k-1)H)\,dA. \tag{9.8}$$

The contribution to this integral from the region between the contours C_{v+dv} and C_v is

$$dW = \oint_C 2\omega^{-1}((H^2 - K)^{\frac{1}{2}} + (k-1)H)\,ds(-dv). \tag{9.9}$$

We require to find a lower bound on this integral. Clearly, since $K \leqslant 0$, the integrand cannot be less than $2k\omega^{-1}H$, where

$$2H = \kappa_t + \kappa_n = (\kappa_t^2 + \kappa_{nt}^2)\,\kappa_t^{-1} + K\kappa_t^{-1} \tag{9.10}$$

using (9.7) to eliminate κ_n. However, since $\kappa_t > 0$ and $K \leqslant 0$, (9.10) does not give a lower bound to H. A stronger inequality is hence required. Returning to (9.9) and using the binomial expansion and the fact that $|K/H^2| \leqslant 1$, it follows that $(H^2-K)^{\frac{1}{2}} \geqslant H-K/2H$, so that the integrand in (9.9) cannot exceed $2\omega^{-1}(kH-K/2H)$. Using (9.10) we can now deduce the stronger inequality:

$$\mathrm{d}W \geqslant \oint_C \omega^{-1}k(\kappa_t^2+\kappa_{nt}^2)\,\kappa_t^{-1}\,\mathrm{d}s(-\mathrm{d}v) - \oint_C \omega^{-1}K\kappa_t^{-1}(\kappa_t+\kappa_n)^{-1}\,(2\kappa_t - k(\kappa_t+\kappa_n))\,\mathrm{d}s(-\mathrm{d}v). \quad (9.11)$$

The second integral can be omitted without violating the inequality, provided $2\kappa_t \geqslant k(\kappa_t+\kappa_n)$. For the simply supported plate this requires $\kappa_n \leqslant \kappa_t$ but for the clamped plate it requires the stronger inequality $\kappa_n \leqslant 0$ in the hyperbolic region.

If these side conditions are met it follows that:

$$-\frac{\mathrm{d}W}{\mathrm{d}v} \geqslant J_1 = k\oint \omega^{-1}\kappa_t(1+\kappa_{nt}^2/\kappa_t^2)\,\mathrm{d}s = k\int_0^{2\pi} \sec^2\eta\,\mathrm{d}\psi = k\int_{C'} q^{-1}\,\mathrm{d}\sigma \quad (9.12)$$

using (8.1) where q is the pedal coordinate and $\mathrm{d}\sigma$ the element of arc length in the hodograph diagram. As already noted in a *parabolic* collapse mode, this integral is identical with $\oint p^{-1}\,\mathrm{d}s$ (cf. equations (5.4) and (8.5)).

In the presence of hyperbolic régimes therefore the inequality in (5.5) is replaced by

$$W \geqslant v_{\mathrm{m}}(J_1)_{\min} \geqslant v_{\mathrm{m}}\,k\left(\oint_{C'} q^{-1}\mathrm{d}\sigma\right)_{\min} \geqslant v_{\mathrm{m}}\left(\frac{B_{\mathrm{h}}^2}{2A_{\mathrm{h}}}\right)_{\min} \quad (9.13)$$

and the conjectured inequality (3.2) is replaced by

$$W/V \geqslant (3k/2)\,(B_{\mathrm{h}}^2/A_0A_{\mathrm{h}})_{\min}, \quad (9.14)$$

where $(B_{\mathrm{h}}^2/A_{\mathrm{h}})_{\min}$ is the minimum value attained by this ratio.

The above argument would suggest, but not prove, that in fact the proposed conjecture is not true when the mechanism is partly hyperbolic, despite having already been shown to hold in the particular case of Fox's solution. Further weight is given to this view by consideration of other types of yield condition.

The expression for the energy dissipation rate/unit area for a Tresca plate is

$$D = \tfrac{1}{2}M(|\kappa_1|+|\kappa_2|+|\kappa_1+\kappa_2|) \quad (9.15)$$

and for a Mises plate is

$$D = (2M/\surd 3)\,(\kappa_1^2+\kappa_2^2+\kappa_1\kappa_2)^{\frac{1}{2}}. \quad (9.16)$$

The corresponding energy dissipatioin rate functionals are hence in general nonlinear. In this respect these yield conditions are analogous to the hyperbolic sections of the square yield condition.

No exact analytic solutions for non-circular Tresca or Mises plates are known. A number of numerical bounding results are available however. The 'natural' generalization of the main *strong* conjecture (1.1) for the square yield locus to a plate with arbitrary yield conditions as suggested by Lowe (1988*c*) is

$$(p/M) \geqslant (B^2/4\pi A)\,(p_c/M), \quad (9.17)$$

PHILOSOPHICAL TRANSACTIONS OF THE ROYAL SOCIETY A MATHEMATICAL, PHYSICAL & ENGINEERING SCIENCES

where p_c is the collapse pressure of the corresponding circular plate, with the same area, boundary support condition and yield locus as the original plate. For a Mises plate with clamped edges $p_c/M = 12.5\pi/A$ (Hopkins & Prager 1953) so that this conjecture predicts a lower bound of $3.125(B^2/A^2) = 44.46/L^2$ for the value of p/M for a clamped square plate of side L. However, Ranaweera & Leckie (1970) have computed an *upper* bound to this ratio of $44.26/L^2$ while Christiansen & Larsen (1983) predict an exact value of $44.13/L^2$. This figure of 44.13 is quoted to an accuracy of ± 0.01; however, as the authors are at pains to point out, this value is obtained by extrapolation from the computed values by letting the mesh size tend to zero, and that there is currently no theoretically established order of convergence for this limit. There must hence still be some doubt about the validity of these computed results. Nevertheless they certainly throw doubt on the validity of the conjecture, at least in this extended form, and this in turn further indicates that the original conjecture may not hold for hyperbolic mechanisms.

10. Conclusions

The *strong* conjecture proposed by Lowe has been established for isotropic plates collapsing according to the square yield criterion provided the mechanism consists of rigid regions and plastically deforming zones which have either elliptic or parabolic curvature. This includes all the known solutions of classical yield-line theory. The conjecture has not been established for mechanisms involving plastic regions with hyperbolic curvature, such as Fox's clamped, square plate solution, and hence cannot be held to be universally true for arbitrary square yield locus mechanisms. The essential difference between the problem for elliptic–parabolic and hyperbolic mechanisms is in the form of the work-rate integral W. For the first class of problems the functional W is linear in the second derivatives of the transverse velocity v and this integral can be expressed as a line integral around the mechanism perimeter. This functional is nonlinear whenever regions of anticlastic curvature occur and cannot be transformed into a boundary integral. It has been shown that the v-contours of a parabolic mechanism always possess a piecewise quadratic A–v relationship and in consequence the required isoperimetric inequality is readily established using the Schwarz transformation and inequality. A very much weaker result has been established for cases where anticlastic curvatures occur which involves the geometry of the dual hodograph diagram.

The work-rate functionals associated with other failure criteria, such as Tresca or von Mises, are in general nonlinear and hence are of the same type as those arising in hyperbolic, square yield condition, mechanisms. The *strong* isoperimetric conjecture would appear to be violated by some numerical solutions for plates failing according to the von Mises condition, although the validity of these results is open to question. This would indicate that although Fox's clamped plate solution does satisfy the proposed conjecture, this may be fortuitous, and that in fact the conjecture may not hold for arbitrary square yield condition mechanisms. This question is still open. It should also be borne in mind that the anticlastic region in Fox's solution occupies less than 10% of the total plate area. It is hence perhaps not surprising that the conjecture is found to hold for this particular solution.

The proof of the conjecture for general elliptic–parabolic modes given here, relies heavily on representing the shapes of the transverse velocity contours (angular velocity trajectories) by their pedal equations. Pedal coordinates arise naturally when describing the kinematics of plate deformations with respect to such contours, since they measure respectively the inclination of, and the normal distance from, the angular velocity vector, cf. (6.3) and (6.7). The pedal distance p is also the integrand of the contour integral for the area enclosed by the contour, and so provides the link between the kinematics of the deforming plate and its isoperimetric properties.

Finally it is worth emphasizing that this 'lower bound theorem' is of a different type to the classical lower bound theorem of limit analysis. Its roots are essentially geometrical rather than mechanical.

References

Allen J. D. 1992 M.E. thesis, University of Auckland, New Zealand.

Bach, C. 1920 *Elastizitat und festigkeit*, 8th edn. Berlin: Springer.

Bandle, C. 1980 *Isoperimetric inequalities and applications*. London: Pitman.

Burago, Yu. D. & Zalgeller, V. A. 1980 *Geometric inequalities*. (Translated from Russian by A. B. Sossinsky.) Springer-Verlag.

Chan, H. S. Y. 1972 The collapse load for reinforced concrete plates. *Int. J. Num. Meth. Engng* **5**, 57–64.

Christiansen, E. 1980 Limit analysis for plastic plates. *SIAM. J. math analysis* **11**, 514–522.

Christiansen, E. & Larsen, S. 1983 Computations in limit analysis for plastic plates. *Int. J. Num. Meth. Engng* **19**, 169–184.

Collins, I. F. 1971 On an analogy between plane strain and plate bending solutions in rigid/perfect plasticity theory. *Int. J. Solids Struct.* **7**, 1057–1073.

Collins, I. F. 1973 On the theory of rigid/perfectly plastic plates under uniformly distributed loads. *Acta Mechanica* **18**, 233–254.

Courant, R. & John, F. 1974 *Introduction to calculus and analysis*, vol. II, Wiley.

De Mar, R. F. 1975 A simple approach to isoperimetric problems in the plane. *Math. Mag.* **48**, 1–12.

Fox, E. N. 1972 Limit analysis for plates: a simple loading problem involving a complex exact solution. *Phil. Trans. R. Soc. Lond.* A **272**, 463–492.

Fox, E. N. 1974 Limit analysis for plates: the exact solution for a clamped square plate of isotropic homogeneous material obeying the square yield criterion and loaded by uniform pressure. *Phil. Trans. R. Soc. Lond.* A **277**, 121–155.

Hodge, P. G. & Belytschko, T. 1968 Numerial methods for the limit analysis of plates. *J. appl. Mech. ASME* **35**, 796–802.

Hopkins, H. G. 1957 On the plastic theory of plates. *Proc. R. Soc. Lond.* A **241**, 153–179.

Hopkins, H. G. & Prager, W. 1953 The load carrying capacity of circular plates. *J. Mech. Phys. Solids* **2**, 1–18.

Hsiung, C.-C. 1981 *A first course in differential geometry*. New York: Wiley.

Hurwitz, A. 1902 Sur quelques applications géométrique des séries de fourier. *Ann. Ecole Norm.* **19**, 357–408.

Johnson, W. 1969 Upper bounds to the load for transverse bending of flat rigid perfectly plastic plates. Part 2. An analogy: slip-line fields for analysing the bending and torsion of plates. *Int. J. Mech. Sci.* **11**, 913–938.

Jones, L. L. & Wood, R. H. 1967 *Yield-line analysis of slabs*. London: Chatto and Windus.

Keller, J. B. 1980 Plate failure under pressure. *SIAM. Rev.* **22**, 227–228.

Lin, T.-P. 1977 Maximum area under constraint. *Math. Mag.* **50**, 32–34.

Lowe, P. G. 1982 *Basic principles of plate theory*. Glasgow: Surrey University Press.

Lowe, P. G. 1984 Isoperimetric inequalities in structural mechanics. In *Proc. 9th ACMSM, Sydney*, pp. 147–151.

Lowe, P. G. 1988*a* Conjectures relating to rigid-plastic plate bending. *Int. J. Mech. Sci.* **30**, 365–370.

Lowe, P. G. 1988*b* Conjectures relating to rigid-plastic plate bending. II. *Int. J. Mech. Sci.* **30**, 869–876.

Lowe, P. G. 1988*c* Isoperimetric inequalities in plate bending mechanics. In *Proc. 11th ACMSM, Auckland*, pp. 317–321.

MCR Special Publication 1965 *Recent developments in yield-line theory*. London: Cement and Concrete Association.

Mansfield, E. H. 1957 Studies in collapse analysis of rigid-plastic plates with a square yield diagram. *Proc. R. Soc. Lond.* A **241**, 311–338.

Mariotte, E. 1686 *Traite du movement des eaux et des autres corps fluids*. Paris: Michallet.

Massonnet, Ch. 1967 Complete solutions describing the limit state of reinforced concrete slabs. *Mag. Concrete Res.* **19**, 13–32.

Morley, C. T. 1965 Ph.D. dissertation, University of Cambridge.

Moseley, H. 1834 *A treatise on mechanics applied to the arts*. London: Parker.

Nielsen, M. P. 1964 Limit analysis of reinforced concrete slabs. *Acta Polytechnica Scandinavica* C_i, 26.

Nielsen, M. P. 1984 *Limit analysis and concrete plasticity*. Prentice-Hall.

Palmer, A. C. 1970 Application of mathematical programming to yield-line analysis. *Mag. Concrete Research* **22**, 227–231.

Payne, L. E. 1991 Some comments on the past fifty years of isoperimetric inequalities. In *Inequalities – fifty years on from Hardy, Littlewood and Polya. Lectures Notes pure appl. Math.* **129**, 143–161 (ed. W. Norrie Everitt). New York: Marcel Decker.

Polya, G. & Szego, G. 1951 *Isoperimetric inequalities in mathematical physics*. Princeton University Press and Oxford University Press.

Prager, W. 1959 *Introduction to plasticity*. Addison-Wesley.

Ranaweera, M. D. & Leckie, F. A. 1970 Bound methods in limit analysis. In *Finite element techniques in stuctural mechanics*, ch. 9, pp. 259–282 (ed. H. Tottenham & C. Brebbia). University of Southampton.

Sawczuk, A. & Hodge, P. G. 1968 Limit analysis and yield line theory. *J. appl. Mech.* **35**, 357–362.

Sawczuk, A. & Jaeger, T. 1963 *Grenztragfahigkeitstheorie der platten*. Berlin: Springer-Verlag.

Shaefer, P. W. 1988 *Maximum principles and eigenvalue problems in partial differential equations*. Harlow, U.K.: Longmans.

Schumann, W. 1958*a* On limit analysis of plates. *Q. appl. Math.* **16**, 61–71.

Schumann, W. 1958*b* On isoperimetric inequalities in plasticity. *Q. appl. Math.* **16**, 309–314.

Singmaster, D. & Souppouris, D. J. 1978 A constrained isoperimetric problem. *Math. Proc. Camb. phil. Soc.* **83**, 73–82.

Sobotka, Z. 1989 *Theory of plasticity and limit design of plates*. Amsterdam: Elsevier.

Strang, G. 1979 A family of model problems in plasticity. Computing methods in applied sciences and engineering. *Springer-Verlag Lecture Notes*, vol. 704 (ed. R. Glowinski & J. L. Lions), pp. 292–308. New York: Springer-Verlag.

Wood, R. H. 1961 *Plastic and elastic design of slabs and plates*. London: Thames and Hudson.

Wood, R. H. 1968 *Engineering plasticity* (ed. J. Heyman & F. A. Leckie), pp. 665–691. Cambridge University Press.

Wood, R. H. 1969 A partial failure of limit analysis for slabs, and the consequences for future research. *Mag. Concrete Res.* **21**, 79–90.

Received 29 April 1992; accepted 8 February 1993

MATHEMATICAL, PHYSICAL & ENGINEERING SCIENCES
PHILOSOPHICAL TRANSACTIONS OF THE ROYAL SOCIETY A